apsis on orbit 2. The ground analysis derives T_e by fitting a theoretical function to the points measured within the exponential portion of the curve (2); N_e is derived from the amplitude of the electron current collected when a fixed positive potential is applied after each curve is obtained (not shown in Fig. 2).

Although the spacecraft travels both horizontally and vertically through the ionosphere, its horizontal uniformity and the eccentricity of the orbit are probably sufficient to permit us to view the measurements in terms of altitude structure. Thus, after the onboard temperatures are normalized to those derived by computer fitting of stored curves, the inbound measurements from two orbits were plotted against altitude in Fig. 3. These orbits were selected to illustrate the ionosphere response to both quiet and disturbed solar wind conditions. Orbit 4 corresponded to a nominal solar wind pressure of 1.9×10^{-8} dyne cm^{-2}, and orbit 9 occurred after a solar flare when the solar wind pressure was 1.8×10^{-7} dyne cm^{-2} (4).

The smooth profiles of orbit 4 suggest that during times of low solar wind pressure direct solar wind heating may be taking place only at the top of the ionosphere. The T_e profile is consistent with the deposition of an energy of 3×10^{10} eV cm^{-2} sec^{-1} at the ionopause, with vertical heat conduction maintaining the steep gradients of T_e observed throughout the ionosphere. This profile is similar to the theoretical ones calculated by Chen and Nagy (5) and Cravens *et al.* (6), which assumed that the ionosphere contains no magnetic field. Since the quiet solar wind energy flux at Venus is probably about 10^{12} eV cm^{-2} sec^{-1}, the observed T_e could be maintained if less than 5 percent of this energy is coupled to the ionosphere. Russell (7) has estimated that 29 percent of the solar wind energy may be absorbed by Venus at times. The more disturbed profiles of orbit 9 illustrate the havoc that was wrought upon the ionosphere by intense solar winds that followed a solar flare on 11 December. The ionopause moved inward, and wavelike structure was evident in both the T_e and N_e profiles.

The various mechanisms for solar wind–ionosphere interactions were reviewed by Michel (8), and more recently by Bauer (9). Most such mechanisms involve a magnetic field induced at the ionopause by compression of solar wind magnetic fields or by currents flowing in the ionosphere itself. Thus it may be instructive to compare the static magnetic field pressure from Pioneer Venus orbiter magnetometer measurements (10) with the static plasma pressures calculated for OETP measurements. In Table 1 we show the calculated plasma pressure at the inner edge of the ionopause, $N_e k\ (T_e + T_i)$, and the magnetic pressure, $B^2/8\pi$, just outside the ionopause for four inbound crossings; B (the local magnetic field strength), N_e, and T_e were measured, and the ion temperature (T_i) was assumed equal to one-half of T_e (11). It is clear that the magnetic pressure balanced the ionospheric pressure within a factor of 2, thus suggesting that the induced magnetic field plays an important role in the transfer of solar wind pressure to the ionosphere.

Large variations in ionopause height and shape have been noted during the 3-week period for which we now have data. Figure 4 records the ionopause heights as a function of solar zenith angle for all orbits available at this writing. The bars indicate the thickness of the ionopause, with the top of the bar indicating the N_e background and the bottom of the bar indicating the knee at the top of the ionosphere. The height of the ionopause varied from 250 to 1000 km, and its thickness varied from a few kilometers to many hundreds of kilometers. The height variation of the ionopause with solar zenith angle, if any, was smaller than the day-to-day variation observed. The behavior was equally variable inbound and outbound. The apparent lack of ionopause height variation with solar zenith angle is perhaps surprising, as the ionopause had been expected to rise near the terminator where solar wind flow is tangential to the ionosphere, thus exerting reduced pressure (12).

L. H. BRACE, R. F. THEIS
J. P. KREHBIEL
NASA/Goddard Space Flight Center, Greenbelt, Maryland 20771
A. F. NAGY, T. M. DONAHUE
Department of Atmospheric and Oceanic Science, University of Michigan, Ann Arbor 48104
M. B. MCELROY
Center for Earth and Planetary Physics, Harvard University, Cambridge, Massachusetts 02138
A. PEDERSEN
European Space Research and Technology Center, Noordwijk, Netherlands

References and Notes

1. L. Colin, *Space Sci. Rev.* **20**, 451 (1977).
2. L. H. Brace, R. F. Theis, A. Dalgarno, *Radio Sci.* **8**, 341 (1973).
3. L. Colin, *Science* **203**, 743 (1979).
4. J. Wolfe, personal communication.
5. R. H. Chen and A. F. Nagy, *J. Geophys. Res.* **83**, 1133 (1978).
6. T. E. Cravens, A. F. Nagy, R. H. Chen, A. I. Stewart, *Geophys. Res. Lett.* **5**, 613 (1978).
7. C. T. Russell, *J. Geophys. Res.* **83**, 625 (1977).
8. F. C. Michel, *Rev. Geophys. Space Phys.* **9**, 427 (1971).
9. S. J. Bauer, in *NASA Spec. Publ. SP-397* (1976), p. 47.
10. C. Russell, R. C. Elphic, J. A. Slavin, *Science* **203**, 745 (1979).
11. W. Knudsen, K. Spenner, R. C. Whitten, J. R. Spreiter, K. L. Miller, V. Novak, *ibid.*, p. 757.
12. J. R. Spreiter, A. L. Summers, A. W. Rizzi, *Planet. Space Sci.* **18**, 1281 (1970).
13. We thank W. R. Hoegy for his programs used for the analysis of volt-ampere characteristics.

16 January 1979

The Polar Ionosphere of Venus Near the Terminator from Early Pioneer Venus Orbiter Radio Occultations

Abstract. *Fourteen profiles of electron density in the ionosphere of Venus were obtained by the dual-frequency radio occultation method with the Pioneer Venus orbiter between 5 and 30 December 1978. The solar zenith angles for these measurements were between about 85° and 92°, and the latitudes ranged from about 81° to 88° (ecliptic north). In addition to the expected decrease in peak electron density from about 1.5×10^5 to 0.5×10^5 per cubic centimeter with increasing solar zenith angle, a region of almost constant electron density above about 250 kilometers was observed. The ionopause height varies from about 300 to 700 kilometers and seems to be influenced by diurnal changes in solar wind conditions. The structures of the profiles are consistent with models in which O_2^+ dominates near the ionization peak and is replaced by O^+ at higher altitudes.*

The Pioneer Venus orbiter mission, described elsewhere in this issue (1), provides an opportunity for the observation of approximately 80 consecutive radio occultations. These observations will eventually provide the means for determining temporal and spatial trends in the ionospheric and atmospheric structure of Venus from the comparisons of profiles derived from adjacent occultations.

Four separate types of measurements can be derived from the analysis of the downlink S- and X-band radio signals from the orbiter: (i) the frequency of each of the two signals is precisely recorded, yielding changes in the Doppler

 0036-8075/79/0223-0765$00.50/0

shift due to refraction in the planetary atmosphere; (ii) the difference between the two downlink frequencies can be computed, yielding an indication of the plasma concentration along the ray path; (iii) the strength of the two signals is measured to determine how much energy is lost through absorption and scattering in the atmosphere at two different frequencies; and (iv) the scintillation of the media. We present here results obtained from only the differenced Doppler data from the phase-locked-loop receivers at Deep Space Net station 14 at Goldstone, California.

The spacecraft orbit is highly eccentric, with a periapsis altitude as low as 150 km and an apoapsis altitude of about 67,000 km. The projections of the orbiter trajectories on a plane normal to the Earth-Venus line of sight are shown in Fig. 1; also shown are the disk of Venus and the position of the terminator at the beginning of the mission. The occultation data reported here were obtained from the entry portion of the first 26 orbits, which occurred between 5 and 30 December 1978 and covered ecliptic northern latitudes ranging from about 81° to 88° (see Table 1). Because the first 80 occultations occur near periapsis, the spacecraft is quite close to the planet and the limb-to-spacecraft distance ranges from about 3600 to 4500 km. The radial velocity of the Earth-spacecraft line of sight relative to Venus is approximately 6.5 km/sec. The latitude-longitude coverage expected from the Pioneer Venus orbiter occultations is presented in Fig. 2.

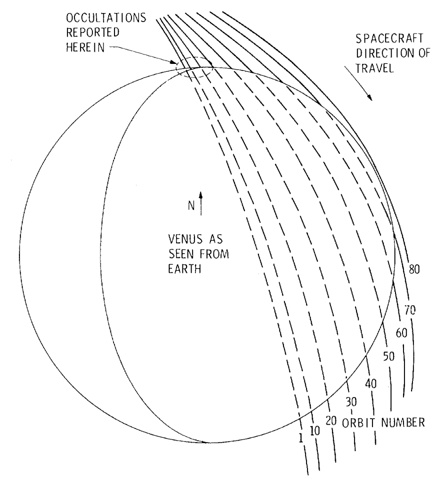

Fig. 1. Projections of the Pioneer Venus orbiter trajectories on a plane normal to the Earth-Venus line of sight (first occultation season).

The orbiter spacecraft, which is described in more detail in (2), contains two features designed specifically for radio science, namely, (i) a coherent X-band transponder and (ii) a despun, two-axis, steerable high-gain antenna which is programmed by commands to follow the direction of the refracted ray throughout each occultation.

The results described here were obtained from 14 of the first 26 occultation entries. The dual-frequency (3) differential Doppler (4) method was used for a combined analysis of the S-band (2294 MHz, 13.06 cm) and X-band (8411 MHz, 3.56 cm) data. The differenced Doppler observable is sensitive only to plasma content along the propagation path, which includes the interplanetary medium and Earth's ionosphere along with the objective of the measurement, the ionosphere of Venus. The small, long-term fluctuations in the differenced Doppler observable caused by effects other than plasma in the ionosphere of Venus are first removed by least-squares fitting a straight line to a portion of the data well outside the Venus ionosphere. Typically, the phase fluctuations in free-space data relative to a straight-line fit show maximum excursions of less than

Table 1. Selected parameters of the Venus polar ionosphere.

Orbit numbers	Date (December 1978)	Solar zenith angle, χ (deg)	Latitude (deg)	Peak altitude, z_p (km)	Peak electron density n_e max ($cm^{-3} \times 10^{-6}$)	Plasma topside scale height (km) Lower H_{p1}	Upper H_{p2}	Ionopause altitude, z_{pl} (km)	Lower peak altitude, z_p (km)	Lower peak electron density, $n_{e_{pl}}$ ($cm^{-3} \times 10^{-4}$)	Remarks
1	5	84.8	80.7	138	1.48	20.4	70.8	~300	125	6.0	"Normal" appearance
3	7	85.2	81.1	141	1.66	18.1	59.9	~700	128	7.2	Unusual "scalloped" structure, 270 to 660 km; three broad peaks of ~3×10^3 cm^{-3}, at ~380, 470, and 590 km
4	8	85.4	81.3	139	1.62	16.3	40.0	~550	126	6.9	"Normal"
5	9	85.5	81.5	141	1.58	16.2	45.1	~500	126	6.8	"Normal"
9	13	86.3	82.4	153*	1.7	18.8	32.5, 52.3	~530	140*	7.8	Vertical ledge at 6.7×10^4 cm^{-3}, 200 to 215 km, day of the solar flare
10	14	86.5	82.7	143	1.55	37.0, 18.3	32.3	~470	127, 113	7.1, 1.6	Ledge at 260 km, constant at 1.1×10^4 cm^{-3}, 230 to 260 km
13	17	87.2	83.7	145	1.38	20.4	131.6, 32.4+	~630	126	6.5	+ Ledge at 260 km, constant at 6.8×10^3 cm^{-3}, 350 to 500 km
14	18	87.5	83.9	145	1.23	13.5	46.7	~450	129	4.7	"Normal" appearance, similar to orbits 1, 3, and 4
17	21	88.3	84.9	145	1.10	18.3	57.1	~450	128	4.1	Ledge at 330 km, constant at 3.2×10^3 cm^{-3}, 330 to 430 km
18	22	88.6	85.2	147	0.97	19.2, 31.3	+	~570	134	4.0	+ Varying between 1×10^3 and 3.2×10^3 cm^{-3}, 250 to 500 km
19	23	88.9	85.6	144	0.87	15.9	+	~560	132	3.5	+ Varying between 2×10^3 and 6×10^3 cm^{-3}, 250 to 550 km
21	25	89.7	86.7	145	0.76	18.6, 35.1	+	~450	129	1.7	+ Varying between 3.2×10^3 and 5×10^3 cm^{-3}, 250 to 430 km
23	27	90.6	87.7	147	0.69	23.7	+	~470	131	2.2	+ Nearly constant at ~ 10^4 cm^{-3}, 230 to 390 km
26	30	91.7	88.3	144	0.52	14.5, 44.3	+	~510	128	1.1	+ Nearly constant at ~3.2×10^3 cm^{-3}, 250 to 430 km

*May not be significant because of uncertainties in the orbit solution introduced by solar activity (10).

0.1 cycle at S-band (1.3 cm), although on days of high solar activity these fluctuations have been observed to increase by about a factor of 5. The data are then inverted by means of the Abel integral transformation method (*5*) to obtain electron density profiles of the Venusian ionosphere. In the inversion technique complete spherical symmetry is assumed, and, although the ray paths are almost parallel to the plane of the terminator, the results show some evidence of asymmetry.

Seven of the profiles, representing orbits 1, 4, 9, 13, 17, 21, and 26, are shown in Fig. 3. This composite of profiles shows graphically the changes in the structure of the ionosphere as the solar zenith angle (χ) changes from 84.8° for orbit 1 to 91.7° for orbit 26. The most obvious change is the appearance of a region of nearly constant electron density between altitudes of about 250 to 500 km in the near-terminator profiles beginning with orbit 17. Some quantitative parameters as well as qualitative remarks describing all 14 of the profiles that were analyzed are given in Table 1. The main ionization peak remains in the range from 138 to 147 km throughout the observation, whereas the peak electron density, which at first ranges from about 1.5×10^5 to 1.7×10^5 cm^{-3}, rapidly begins to decrease when χ falls below 87° and reaches a value of about 5×10^4 cm^{-3} at a χ of 91.7°. There is also in every case a subsidiary lower peak which ranges in altitude from about 125 to 134 km and which decreases in density from about 7×10^4 cm^{-3} for the initial orbits to about 10^4 cm^{-3} for the measurement for orbit 26.

The plasma scale heights computed from these electron density profiles are quite variable from day to day, suggesting considerable diurnal variability in the plasma temperature above the maximum of ionization. In Table 1, two values of the topside plasma scale height are given, the lower and the upper scale height, because in most of the profiles at least two distinct regions of constant scale height are discernible. The lower scale height, ranging from 13.5 to 37 km, probably represents a region in which O_2^+ is the dominant ion. The upper scale heights are even less consistent than the lower scale heights, ranging in value from 32.4 to 70.8 km, and may represent regions in which O^+ is dominant. Since there is evidence that the regions of the ionosphere between 140 and 220 km are covered by chemical rather than diffusive equilibrium (*6*), these scale heights cannot be directly interpreted in terms of plasma temperatures. They are related to neutral temperatures, but assumptions regarding the ionization process must be made in order to establish quantitative relationships.

The ionopause altitude, interpreted here as the height at which the electron density reaches the noise level of these measurements (typically from 10^2 to 10^3 cm^{-3}) has been quite variable, ranging from about 300 to 700 km. In most cases the ionopause appears to be in the range of 450 to 550 km and appears to be governed more by diurnal changes in the solar wind conditions than by the changing χ.

The electron density profiles obtained from orbits 1 through 5 appear qualitatively similiar to profiles obtained from Mariner 5 (*4*) and Mariner 10 (*7*). These profiles, which also compare well with those obtained from Venera 9 and Venera 10 (*8*), show a constant gradual decrease in the electron density. Instead of a sharply defined ionopause, there is a gradual blending of the measured density with the free-space noise level. This then can be interpreted as the typical behavior of the daytime ionosphere at values of χ below about 86° to 87°. When χ becomes greater and the solar illumination becomes more and more horizontal, there appears a region of very slowly changing electron density above 250 km which continues for 200 to 300 km and terminates in a sharply defined ionopause boundary. All of the electron density profiles taken at values of χ over 88° showed this property (see Fig. 3 and the remarks column of Table 1), which is also evident in a profile taken by Venera 9 at a χ of 83° (*8*). Such an extended profile, featuring nearly constant electron densities to the ionopause, is probably characteristic of the daytime ionosphere of Venus near the terminator.

The structures of the electron density profiles compare well with the current models of the atmosphere of Venus (*6, 9*) in which O_2^+ dominates near the ionosphere peak and is replaced by O^+ at higher altitudes. These models are supported by the observation of two regions of constant scale height above the ionization peak with the scale heights differing by roughly a factor of 2.

Future Pioneer orbiter radio occultations will make possible many measurements of the nighttime ionosphere of Venus during the first occultation season

Fig. 2. Expected latitude and longitude coverage of the Pioneer Venus orbiter occultations. The squares denote entries and the triangles exits. Every fifth occultation is plotted for the first occultation season (orbits 1 through 75), and every occultation is shown for the second season (orbits 153 through 164).

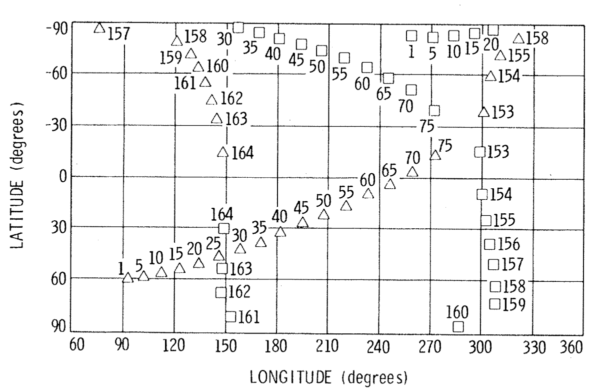

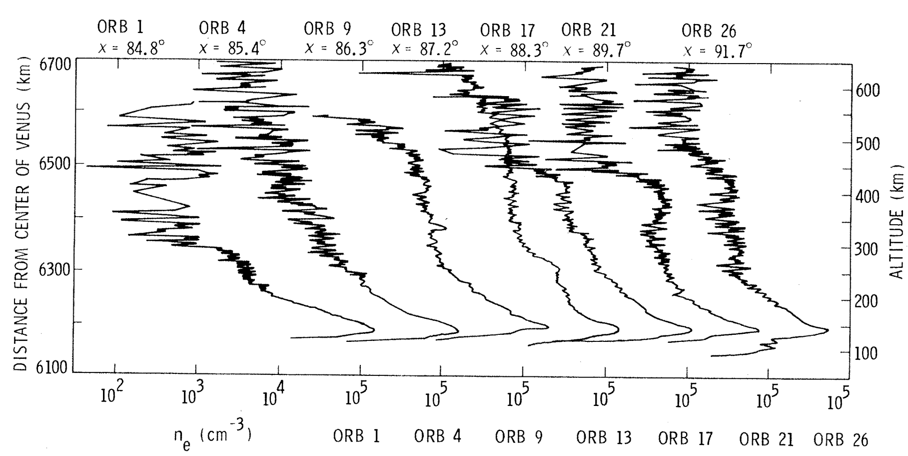

Fig. 3. Electron density profiles (n_e) from entry measurements of orbits 1, 4, 9, 13, 17, 21, and 26. The profiles are staggered by one decade, and the 10^5 cm^{-3} level is indicated for each profile. The solar zenith angle (χ) for each orbit is indicated on the upper horizontal axis.

ending in February 1979. During the extended mission in the fall of 1979 over 100 profiles of the daytime ionosphere at various values of χ will be obtained.

ARVYDAS J. KLIORE, RICHARD WOO
JOHN W. ARMSTRONG, INDU R. PATEL
Jet Propulsion Laboratory, California Institute of Technology, Pasadena 91103

THOMAS A. CROFT
SRI International, Menlo Park, California 94025

References and Notes

1. L. Colin, *Science* **203**, 743 (1979).
2. ——— and C. F. Hall, *Space Sci. Rev.* **20**, 283 (1977).
3. V. R. Eshleman, P. B. Gallagher, R. C. Barthle, *J. Geophys. Res.* **65**, 3079 (1960).
4. G. Fjeldbo and V. R. Eshleman, *Radio Sci.* **4**, 879 (1969).
5. ———, *Planet. Space Sci.* **76**, 123 (1968); A. J. Kliore, in *Mathematics of Profile Inversion*, L. Colin, Ed. (Publication TMX-62, 150, National Aeronautics and Space Administration, Washington, D.C., 1972), p. 3-2.
6. R. H. Chen and A. F. Nagy, *J. Geophys. Res.* **83**, 1133 (1978).
7. G. Fjeldbo, B. Seidel, D. Sweetman, T. Howard, *J. Atmos. Sci.* **32**, 1232 (1975).
8. G. S. Ivanov-Cholodny *et al.*, preprint of paper No. D.2.4, Twenty-first COSPAR meeting, Innsbruck, Austria (Academy of Sciences of the U.S.S.R., Institute of Radio Engineering and Electronics, Moscow, 1978).
9. S. J. Bauer and R. E. Hartle, *Geophys. Res. Lett.* **1**, 7 (1974); S. Kumar and D. M. Hunten, *J. Geophys. Res.* **79**, 2529 (1974).
10. The normal uncertainty (three standard deviations) in the time of closest approach of orbit solutions is about 0.03 to 0.06 second, corresponding to an uncertainty in the altitudes of the electron density profiles of about 0.2 to 0.4 km. Because of the effects on the solar flare activity of 13 December 1978, the corresponding uncertainty for orbit 9 is about 0.9 second, leading to an altitude uncertainty of about 6 km.
11. We thank the many people whose contributions were essential to the success of the radio occultation experiment. The following Pioneer Project, Jet Propulsion Laboratory, and Deep Space Network personnel deserve our special gratitude: C. F. Hall, J. Dyer, J. Cowley, and R. Ramos of NASA Ames Research Center for their design and execution of the mission; R. B. Miller, R. Elwood, W. Hietzke, J. Wackley. D. W. Johnston, and T. Howe of the DSN for their valuable support; W. E. Kirhofer, R. Jacobsen, B. Williams, and T. Lubeley of the JPL Pioneer navigation team for providing us with trajectories as well as predictions for the occultation data recording; P. Laing for the occultation prediction software; and G. H. Pettengill, the leader of the radio science team. We also thank A. F. Nagy for his valuable comments. This work was performed at the Jet Propulsion Laboratory, California Institute of Technology, under NASA contract NAS 7-100.

16 January 1979

Venus Thermosphere: In situ Composition Measurements, the Temperature Profile, and the Homopause Altitude

Abstract. *The neutral mass spectrometer on board the Pioneer Venus multiprobe bus measured composition and structural parameters of the dayside Venus upper atmosphere on 9 December 1978. Carbon dioxide and helium number densities were 6×10^{9} and 5×10^{6} per cubic centimeter, respectively, at an altitude of 150 kilometers. The mixing ratios of both argon-36 and argon-40 were approximately 80 parts per million at an altitude of 135 kilometers. The exospheric temperature from 160 to 170 kilometers was 285 ± 10 K. The helium homopause was found at an altitude of about 137 kilometers.*

The primary objectives of the neutral mass spectrometer (BNMS) experiment on board the Pioneer Venus multiprobe bus were to study the composition and temperature of the Venus upper atmosphere. Of particular interest were measurements near the homopause and the ionospheric peak. The bus passed the 200-km level of the Venus thermosphere on 9 December 1978 at 40°S celestial latitude, at a local solar time of 0835 hours and a local solar zenith angle of 60°. Although it descended through the atmosphere at a rather shallow angle the verticle velocity component of the bus was still 1.4 km per second at the 150-km level where the atmospheric pressure scale height was about 6 km.

The BNMS (*1*, *2*) included a semiopen electron impact ion source, double-focusing analyzing fields, four ion detectors (two multipliers and two electrometers), two pumps, and an in-flight calibration system. The combination of electrometers and ion-counting multipliers together with differential pumping between ion source and analyzing fields made it possible to measure particle densities over eight orders of magnitude. Only the maxima of selected mass peaks were sampled for each 0.1 second. The mass numbers chosen included those expected on the basis of our pre-Pioneer Venus knowledge of the composition of the Venus atmosphere as well as masses associated with anticipated impurities.

Table 1. Temperatures as derived from the measured CO_2 profile.

Altitude (km)	Temperature (K)
200	284
180	281
160	269
150	253
140	221

Table 2. Altitude levels (in kilometers) on dayside of terrestrial planets (*7*).

Level	Venus	Earth	Mars
Exobase	~180	~500	~185
Ionospheric peak	142	270	132
Homopause	137	105	125

As the bus approached Venus, the first gas to be detected was helium at an altitude of about 700 km. Upon sensing a predetermined level of the mass 28 signal the instrument switched automatically to a special low-altitude mass program at 206 km. Data were obtained down to an altitude of approximately 130 km where the ion source operated in the 10^{-3} mbar pressure range. Figure 1 shows particle density profiles for CO_2 and He. The altitude values are preliminary, but are believed to be accurate to 3 km below an altitude of 250 km.

The mass 44 signals started to rise rapidly below 300 km with a gradient that increased down to 200 km; at this altitude the gradient stabilized, at a value corresponding to a scale height of approximately 6 km. The smaller slope above 200 km is tentatively attributed to the contribution of impurities at the mass 44 position, possibly CO_2 produced by the reaction of ambient atomic oxygen with contaminants on the instrument surfaces. Below 200 km, however, the ambient CO_2 becomes the dominant contributor to the mass 44 peak, the impurity effect becoming negligible.

The smoothed CO_2 density profile was used to derive a temperature for the upper thermosphere and exosphere (see Table 1). Our "low" dayside exospheric temperature of 285 K agrees fairly well with that obtained from the orbiter (*3*) and by the ultraviolet spectrometer on Mariner 10 (*4*). The value is close to that predicted by the low-heating-efficiency model of Dickinson and Ridley (*5*). However, it emphasizes that the exosphere temperature, T_{ex}, cannot be obtained from the topside scale height of the ionosphere unless the ratio of oxygen atoms to CO_2 molecules is known.

The instrument He sensitivity was successfully calibrated in flight 2 days before the bus entered the Venus thermosphere. This enables us to place considerable confidence in the absolute He number densities reported here. At 145 km our absolute density is a factor of 3 greater than that found by Kumar and Broadfoot (*4*). At 135 km our ratio for $n(He)/n(CO_2)$, where n is the total number density, is about 130 ppm and is still decreasing toward lower altitudes. The 10 ppm mixing ratio derived by Kumar